HAWC2 v13.1 and HAWCStab2 v2.16 Comparison

Verelst, David Robert; Pirrung, Georg; Riva, Riccardo

Link to article, DOI:
10.11581/DTU.00000323

Publication date:
2024

Document Version
Publisher's PDF, also known as Version of record

HAWC2 v13.1 and HAWCStab2 v2.16 Comparison

DTU Wind

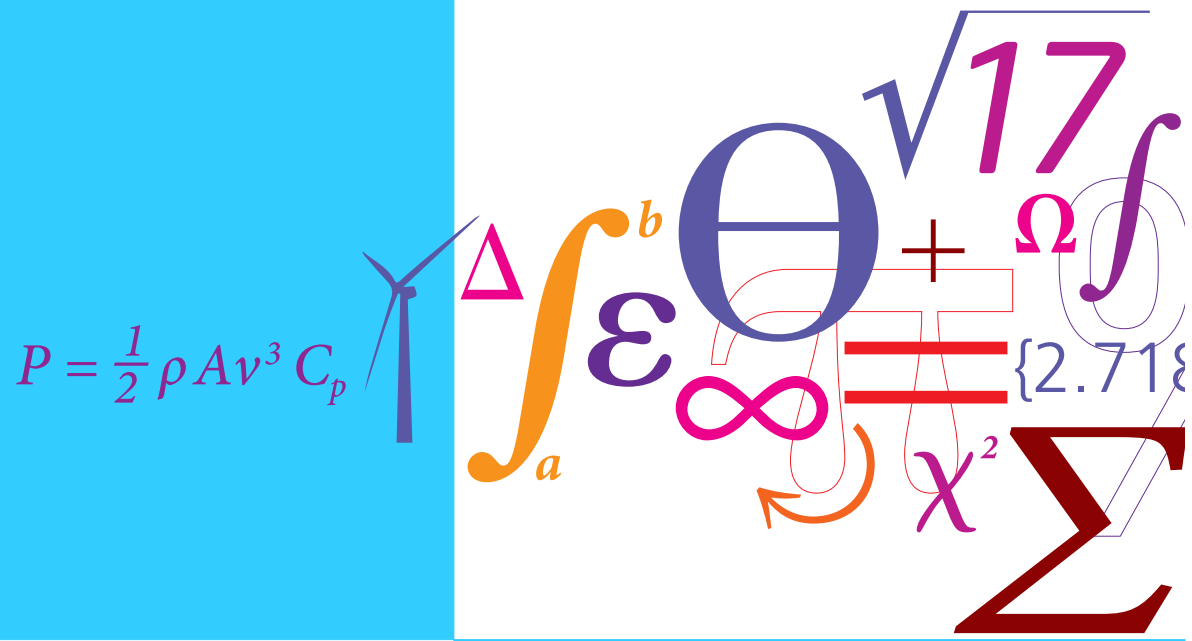

David Verelst, Georg Pirrung, Riccardo Riva
DOI: 10.11581/DTU.00000323

April 2024

DTU Wind Energy
Department of Wind Energy

Contents

1 Introduction

This reports presents comparison of the steady state HAWC2 [1, 2, 3] simulation results and the HAWCStab2 computations of the DTU 10 MW reference turbine [4], as well as a comparison of structural blade-only frequencies and damping ratios. It serves as a simple verification study of the HAWCStab2 [5, 6, 7] computations.

The steady state comparison is shown in Section 2. For a fair comparison, the following simplifications of the DTU 10 MW reference turbine are made:

- no gravity;
- shaft tilt angle is set to zero, since HAWCStab2 assumes the inflow is perpendicular to the rotor plane;
- uniform aligned inflow conditions (no turbulence, shear, veer or yaw);
- tower and shaft flexibility are not considered to assure the shaft remains perfectly aligned with the wind inflow vector (horizontal).

Furthermore, each main-body in the HAWC2 model must contain as many bodies as elements, to be equivalent to the co-rotational formulation used by HAWCStab2.

There are four test cases considered in the steady state comparison:

- Case 1: no blade flexibility, and the aerodynamic modelling reduced to strip theory: no induction and no tip correction, labelled as "no induction" or "without induction".
- Case 2: no blade flexibility in conjunction with BEM induction model and Prandtl tip correction (labelled as "induction+tip").
- Case 3: flexible blades in conjunction with "induction+tip". Includes power and thrust curve comparison with HAWCStab2 2.15.
- Case 4: flexible blades in conjunction with "induction+tip", 15 degrees coning. Includes power and thrust curve comparison with HAWCStab2 2.15.

Both HAWC2 and HAWCStab2 have the ability to use different aerodynamic models. For the "induction+tip" model, the rotor induced velocities are calculated with Blade Element Momentum theory, and the presence of the tip vortex is accounted for by the Prandtl tip loss model. For not completely planar rotors, for example due to cone or blade deflection, a component of the rotor rotation is a rotation of the aerodynamic cross sections about the local blade axis (often referred to as a pitch rate or torsion rate). Furthermore, there will be a centripetal acceleration of the airfoil cross sections due to the rotor rotation, that causes added mass lift and drag components. These effects and their modelling are described in [8]. The corresponding terms are included in the HAWCStab2 steady state computations since version 2.16. Because the terms are part of the unified dynamic stall model in HAWC2, dynamic stall in HAWC2 is active in all comparisons to ensure the correct steady state results.

Section 3 contains a comparison of the structural blade-only frequencies and damping ratios. The comparisons are performed using the classical beam model and the FPM model, as well as the damping_posdef and damping_aniso_v2 commands.

This investigation has been carried out with HAWC2 version 13.1 and HAWCStab2 version 2.16. Previous iterations of this report compared HAWC2 version 12.2 with HAWCStab2 2.12 [9] and HAWC2 version 12.5 vs HAWCStab2 2.14 [10].

2 Steady state results

This comparisons of the steady state results of the DTU 10 MW considers the following integrated rotor performance parameters, as function of wind speed:

- mechanical rotor power;
- rotor thrust.

The following distributed blade performance parameters are considered:

- The z-coordinate of the blade section (in blade coordinates) on the x-axis
- Lift and drag coefficients (Cl and Cd respectively).
- Angle of attack (AoA).
- Relative velocity as seen from the blade section (vrel).
- Distributed lateral and axial forces (F_x and F_y respectively) in rotor polar coordinates.
- Axial and tangential induced velocities (ax_ind_vel and tan_ind_vel).

2.1 Case 1: stiff blades and “no induction”

This is the most basic and simple comparison possible: an entirely stiff structure, steady and uniform inflow conditions, and basic strip theory for the aerodynamics (no induction, nor tip correction). From the power curve given in Figure 2.1 it can be noted that in the absence of deflections, and without the proper aerodynamic model, the nominal power is significantly over estimated.

From Figure 2.1 is noted that the difference between HAWC2 and HAWCStab2 is very small:

- maximum difference on power output is 80 kW (roughly 0.4% at ≈ 20 MW);
- maximum difference on thrust is 0.6 kN (roughly 0.08% at 800 kN).

These differences are considered very small and are argued to be caused by the small differences in numerical integration schemes used for integrating the rotor forces.

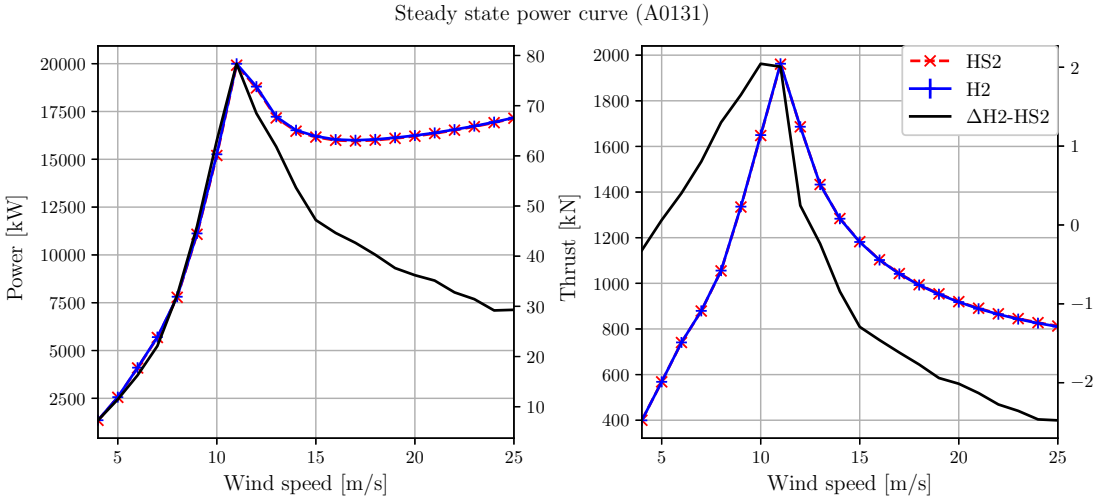

Figure 2.1: Power and thrust curves. The absolute difference between HAWC2 and HAWCStab2 is labelled as ΔH2-HS2, and its axis is on the right side of the plot.

Figures 2.2 to 2.5 consider the blade distributed aerodynamic parameters. For the fully stiff case with simple aerodynamics the distributed forces compare very well between HAWC2 and HAWCStab2. The minor differences that occur are mainly located within the inner part of the blade. Notice that the induced velocities are zero since the induction model is switched off.

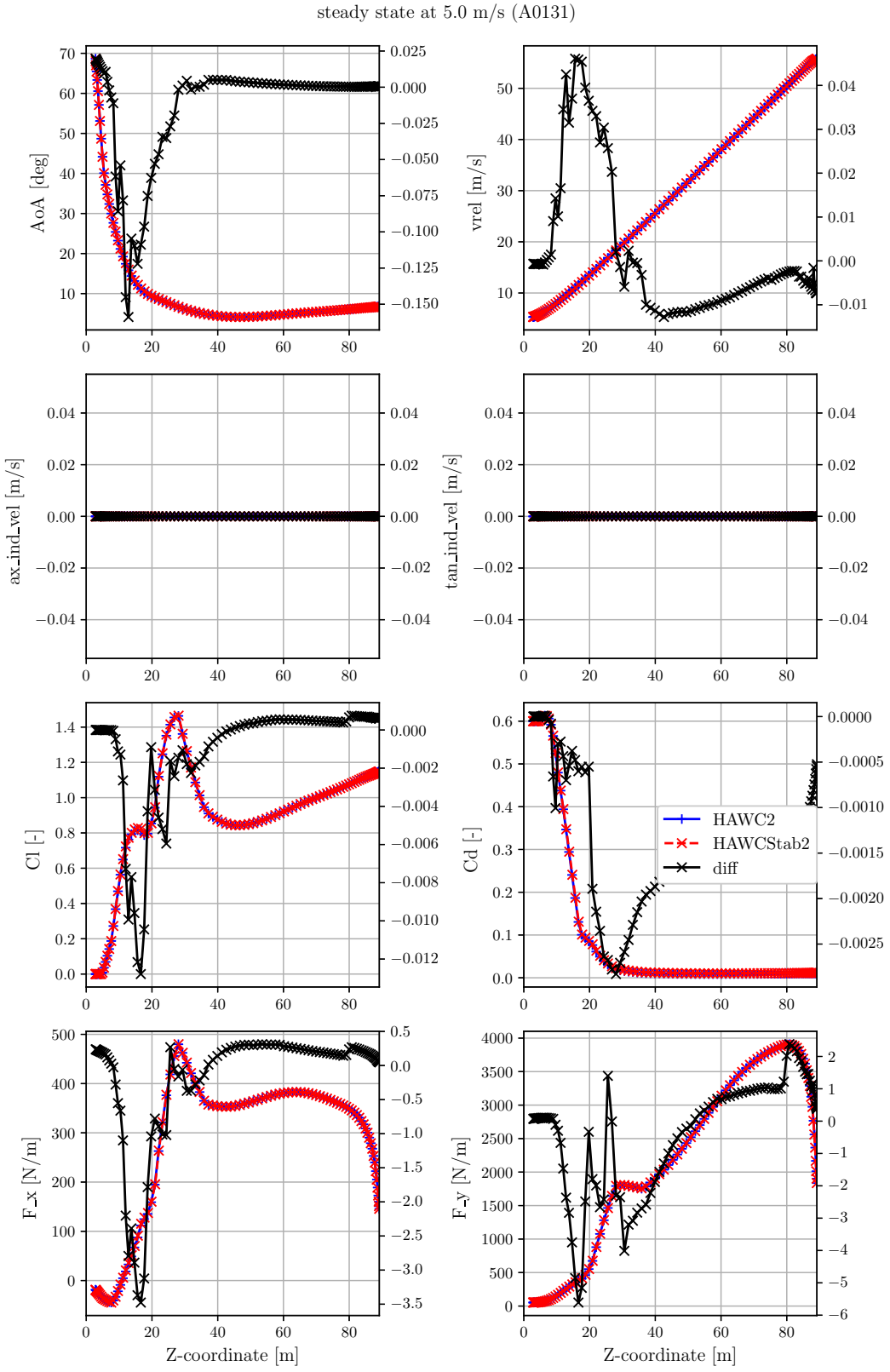

Figure 2.2: Blade load distribution at 5 m/s. The absolute difference between HAWC2 and HAWCStab2 is labelled as *diff*, and its axis is on the right side of the plot.

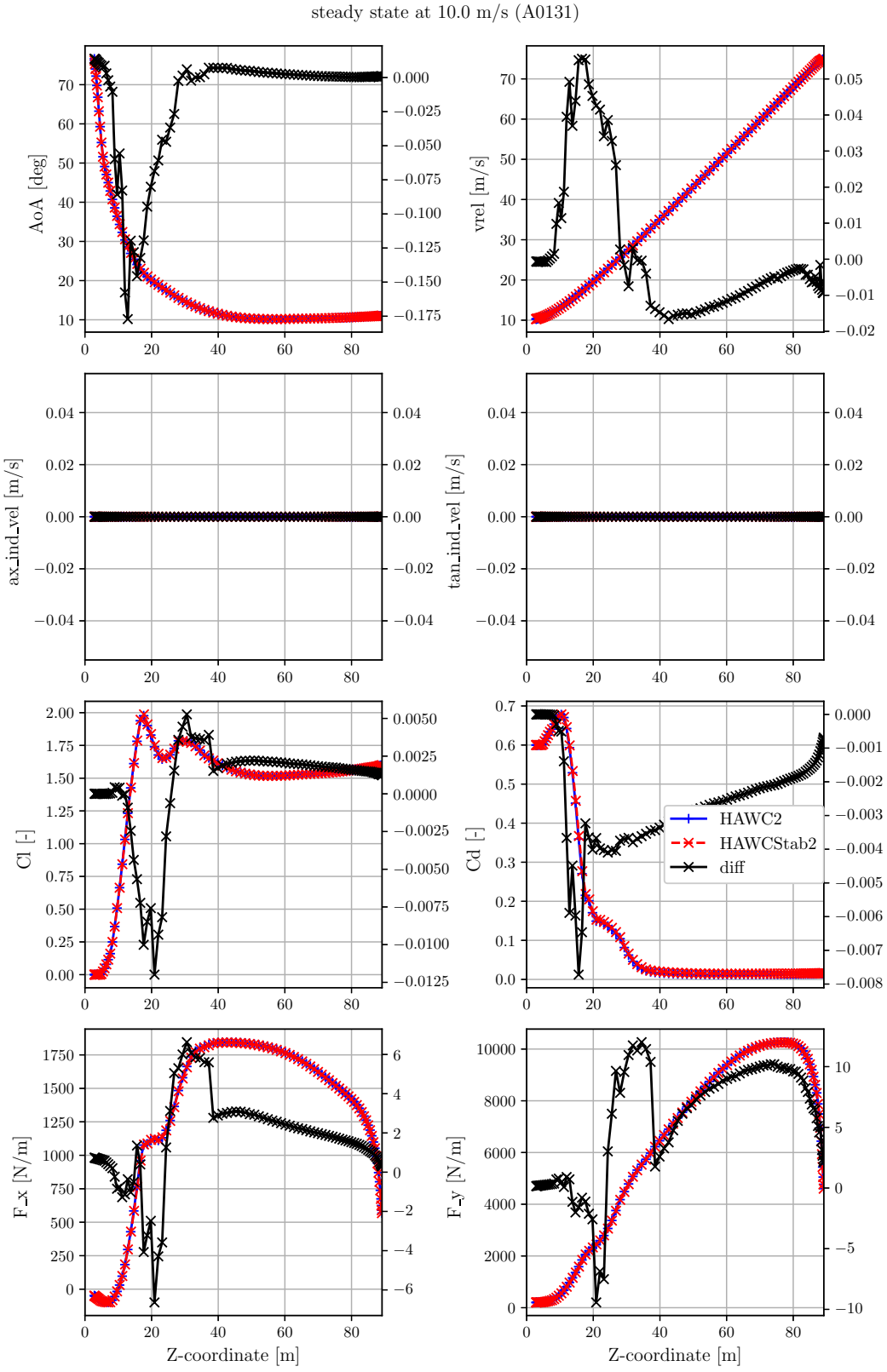

Figure 2.3: Blade load distribution at 10 m/s

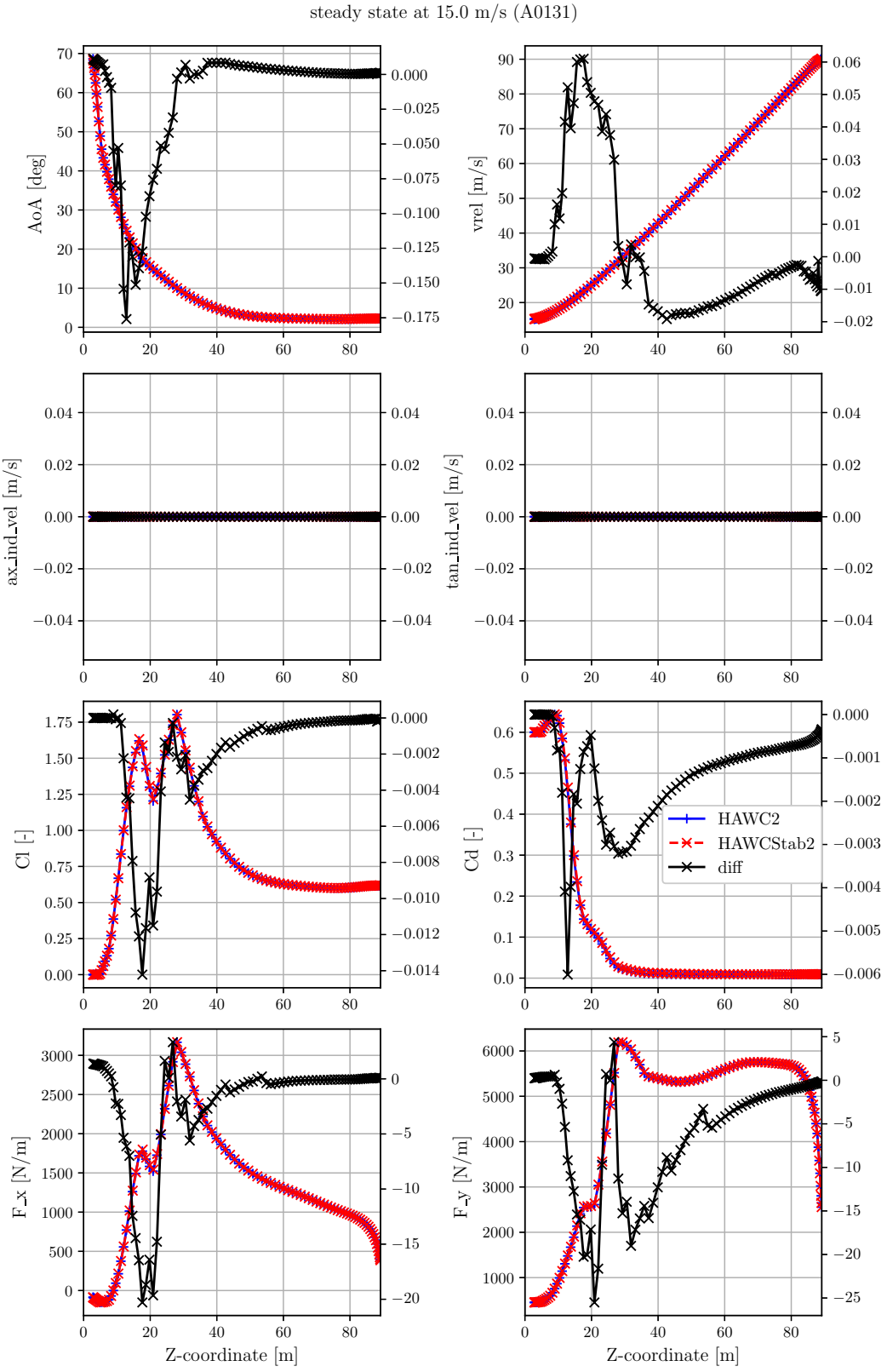

Figure 2.4: Blade load distribution at 15 m/s

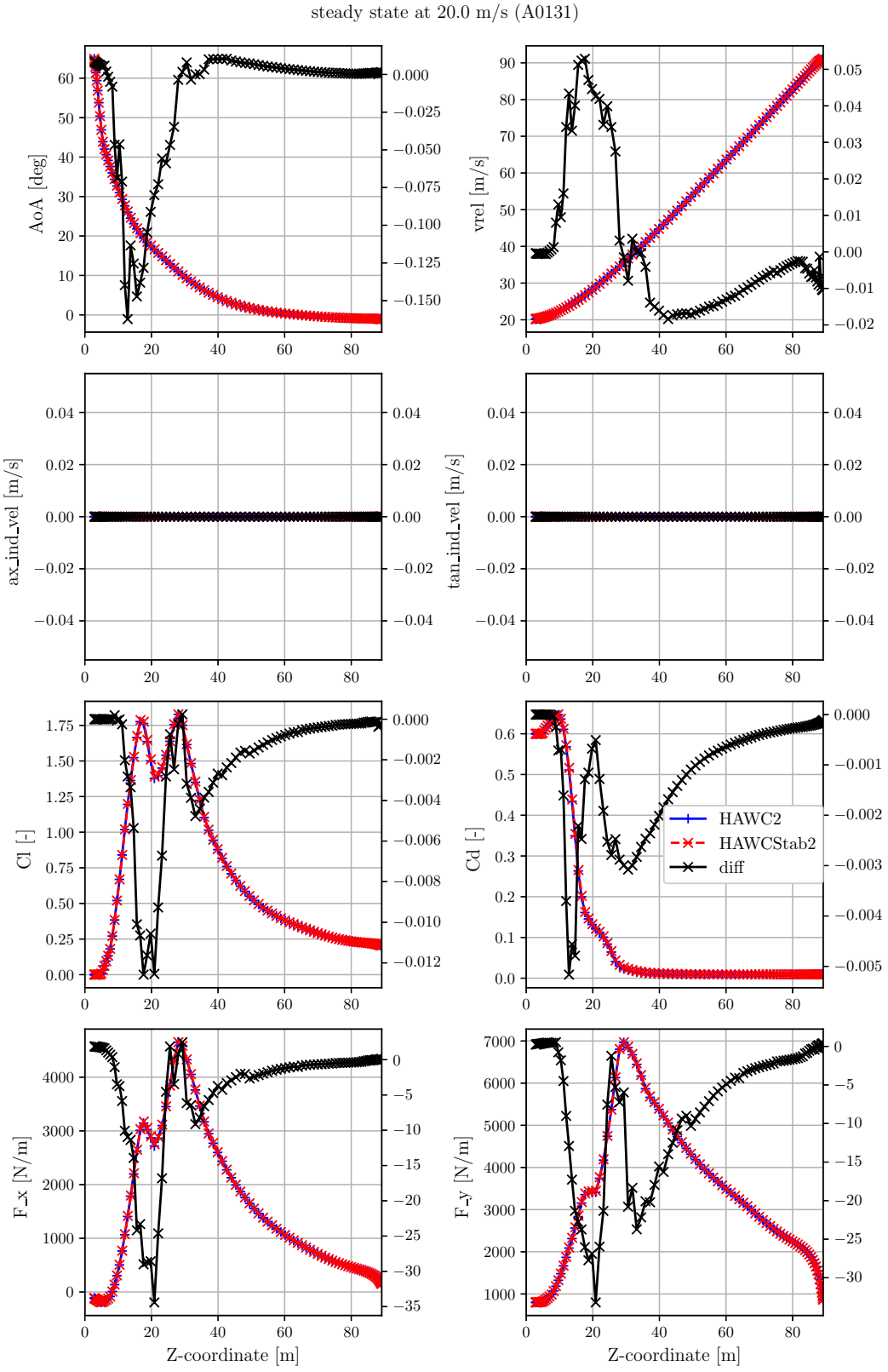

Figure 2.5: Blade load distribution at 20 m/s

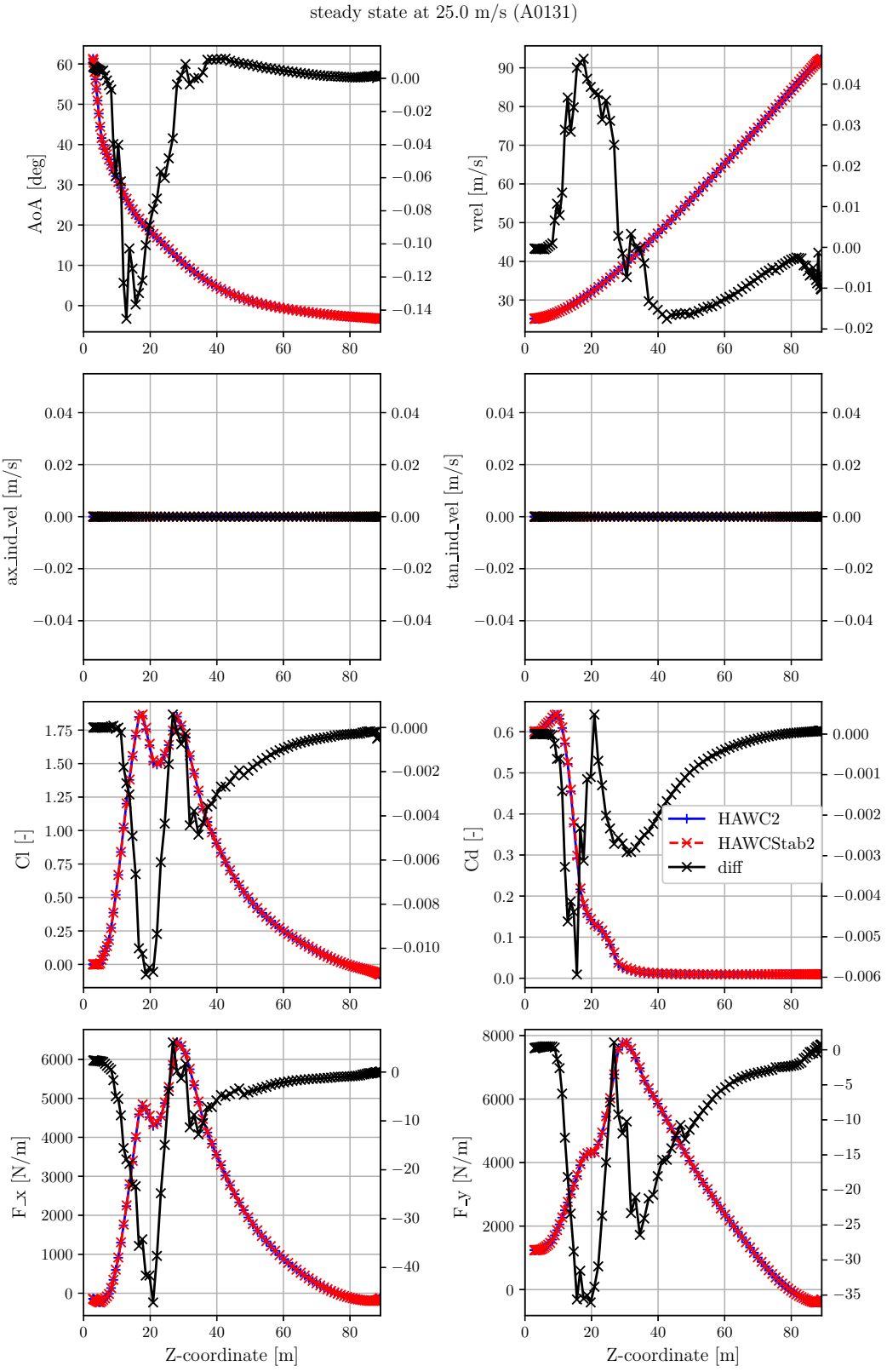

Figure 2.6: Blade load distribution at 25 m/s

2.2 Case 2: stiff blades and “induction+tip”

When using a more realistic aerodynamic model, but still stiff blades, the good agreement between HAWC2 and HAWCStab2 still holds. The integrated forces are shown in Figure 2.7 in the form of the power and thrust curves as function of wind speed. The error between HAWC2 and HAWCStab2 remains well below 1%.

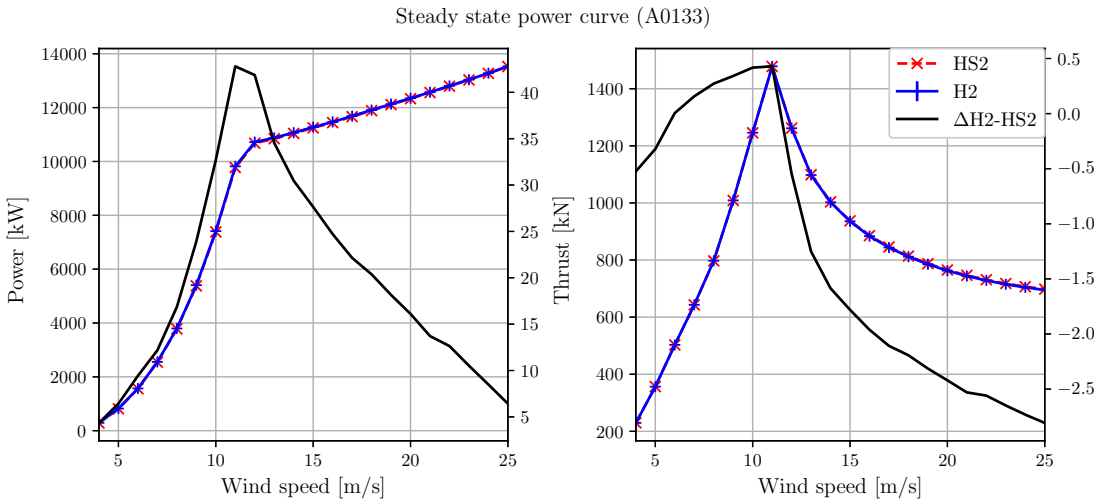

Figure 2.7: Power and thrust curves. The absolute difference between HAWC2 and HAWCStab2 is labelled as ΔH2-HS2, and its axis is on the right side of the plot.

The distributed aerodynamic parameters (Figures 2.8 to 2.12) show a very good agreement between both codes. However, following minor differences are observed:

- The same minor differences are occurring at the inner part of the blade compared to case 1.
- At the tip a very small discrepancy exists due to presence of the tip loss model. A more detailed assessment as of why the tip loss model causes this difference is referred to future work.

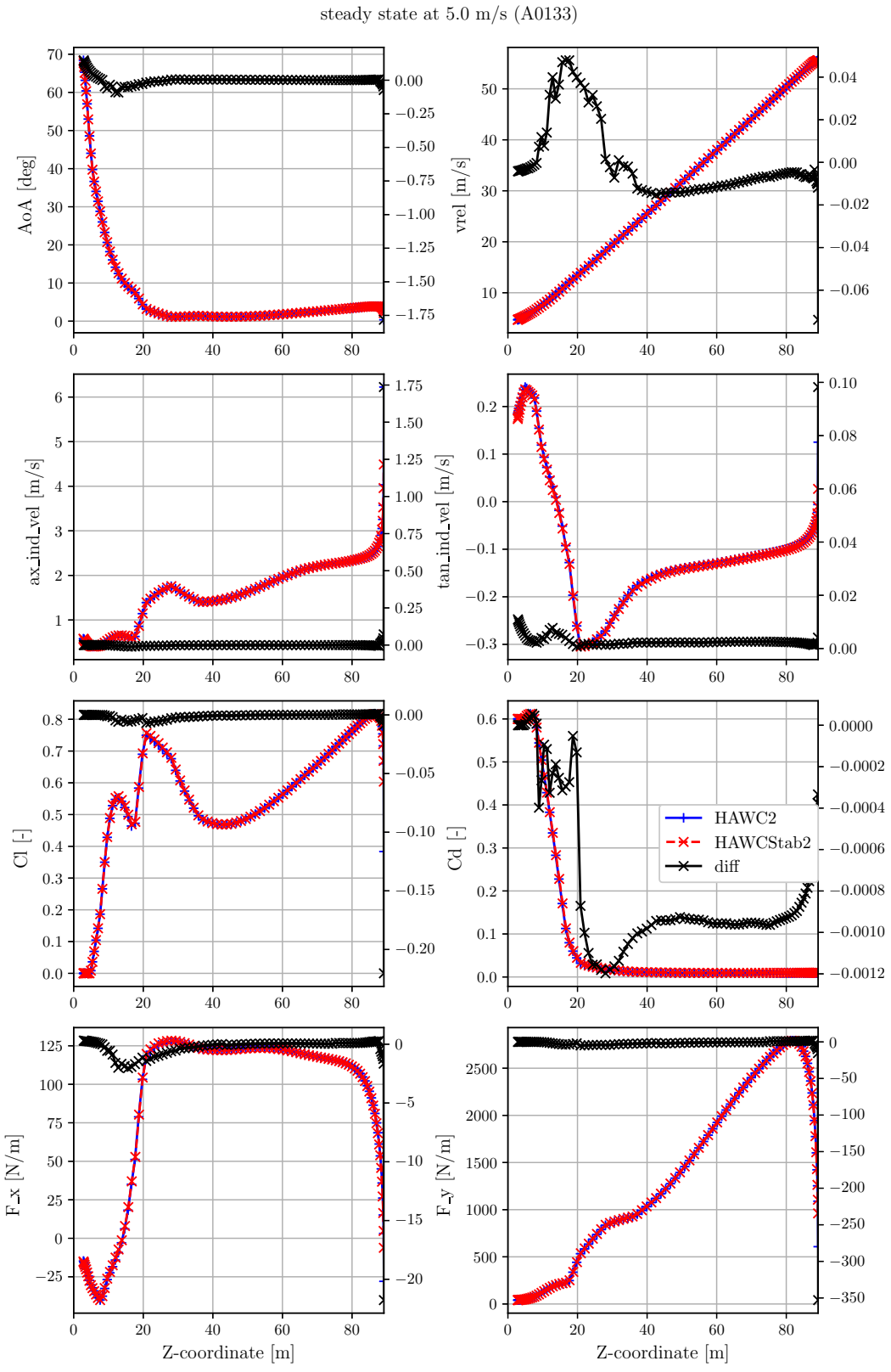

Figure 2.8: Blade load distribution at 5 m/s.

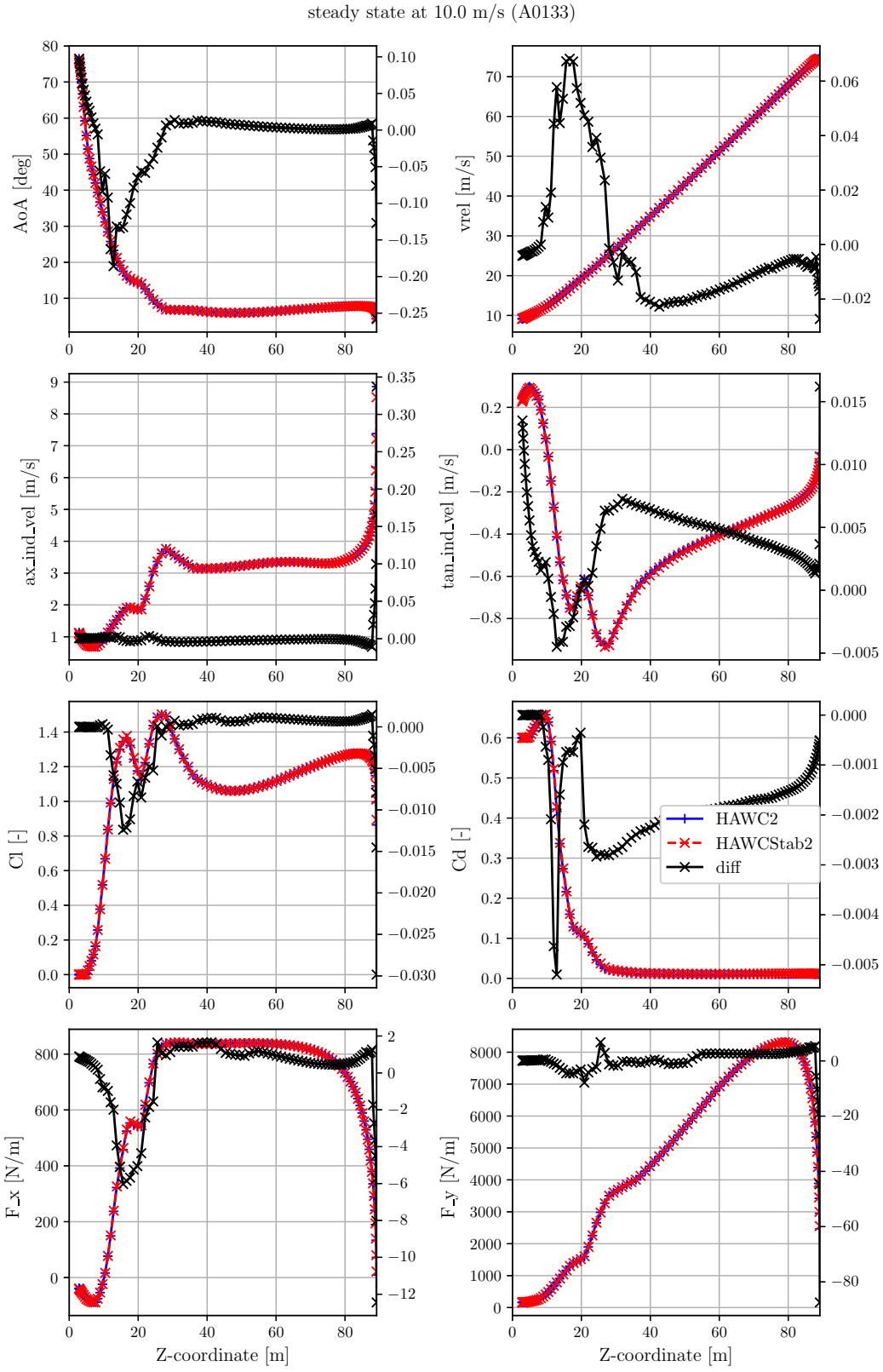

Figure 2.9: Blade load distribution at 10 m/s.

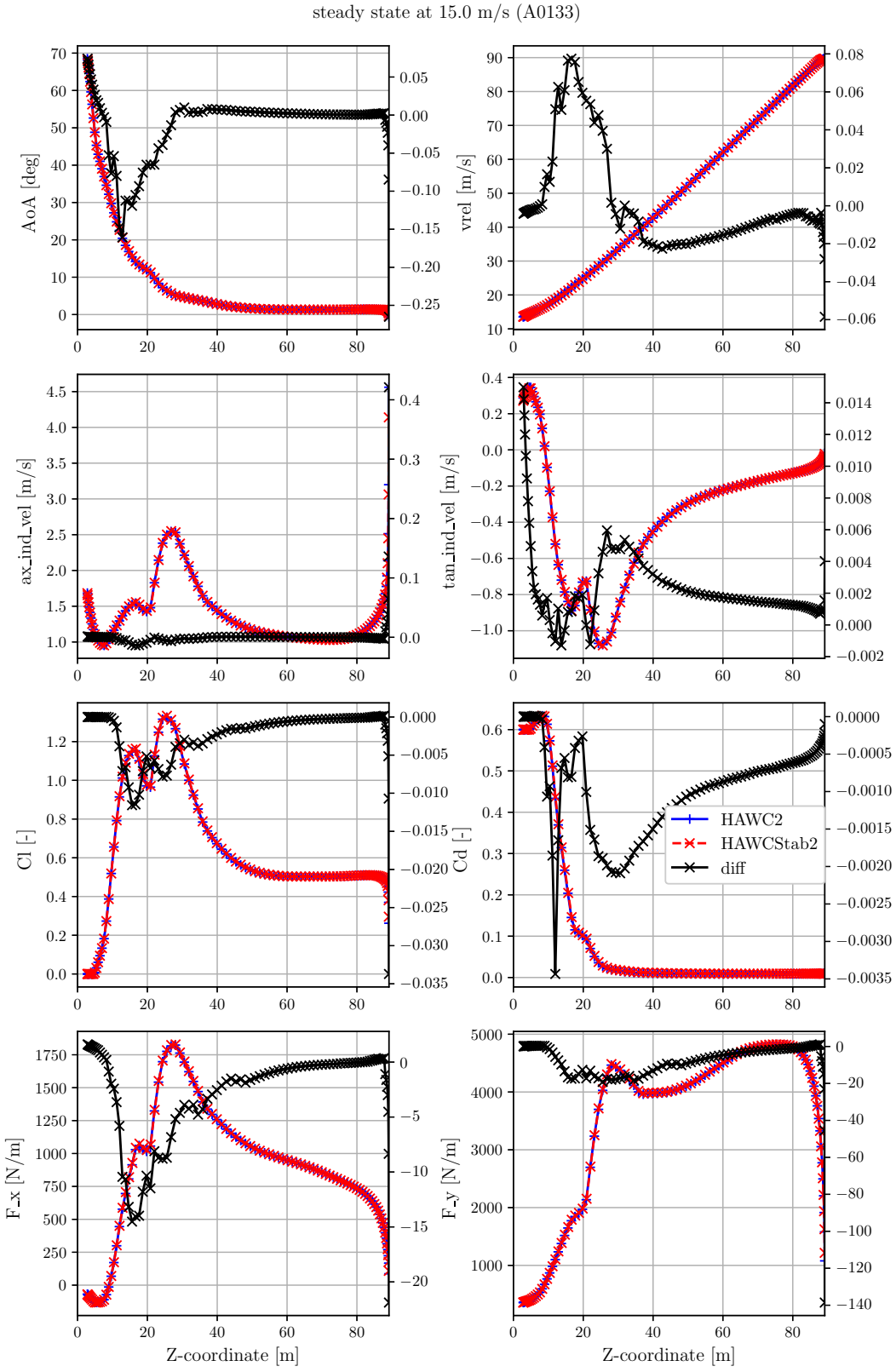

Figure 2.10: Blade load distribution at 15 m/s.

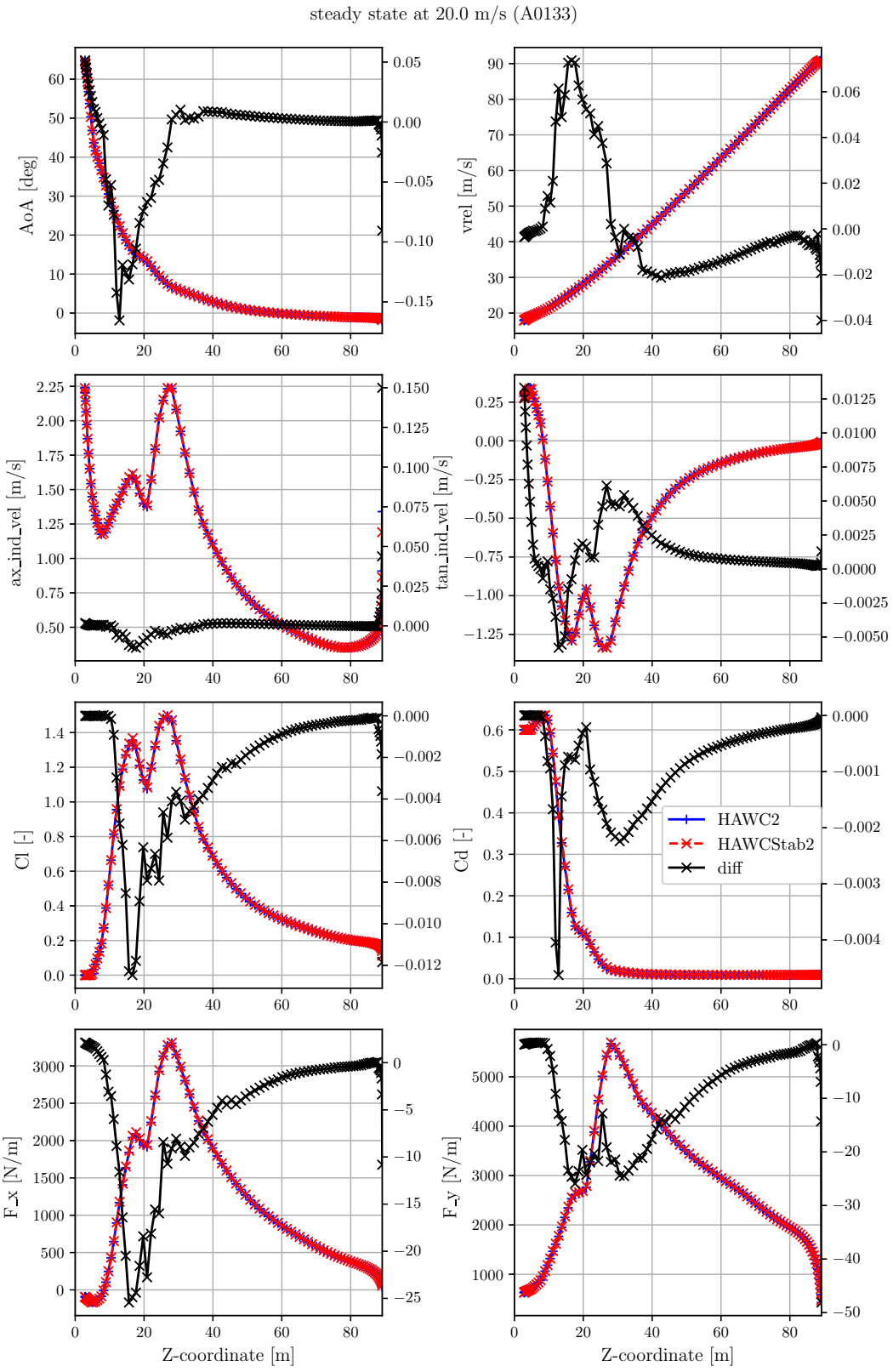

Figure 2.11: Blade load distribution at 20 m/s.

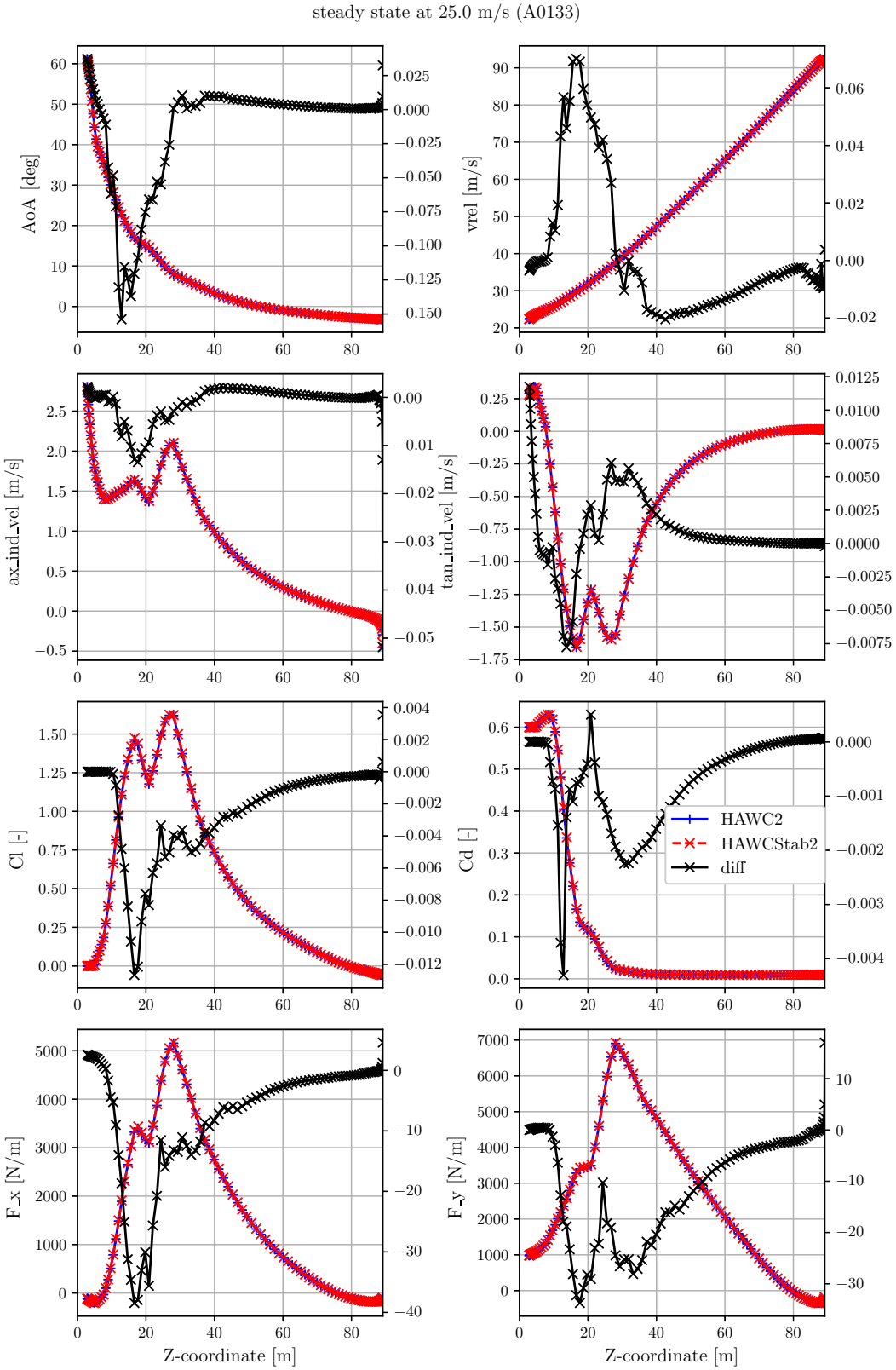

Figure 2.12: Blade load distribution at 25 m/s.

2.3 Case 3: flexible blades and “induction+tip”

When considering both the “BEM+tip aerodynamic” model and blade flexibility the same consistent and good agreement between both HAWC2 and HAWCStab2 is found. This for both integrated power and thrust (see Figure 2.13 and distributed aerodynamic parameters (Figures 2.14 to 2.17).

Once again, HAWCStab2 2.16 compares well with HAWC2 13.1, as can be seen by the black, solid, line in Figure 2.13. HAWCStab2 2.15 produced equivalent results to HAWC2 12.6, which used an older aerodynamic model and that is why the black, dashed, line shows a large discrepancy. Updating the aerodynamics in HAWCStab2 reduced the largest absolute power deviation by roughly a factor of 10 in version 2.16 compared to 2.15.

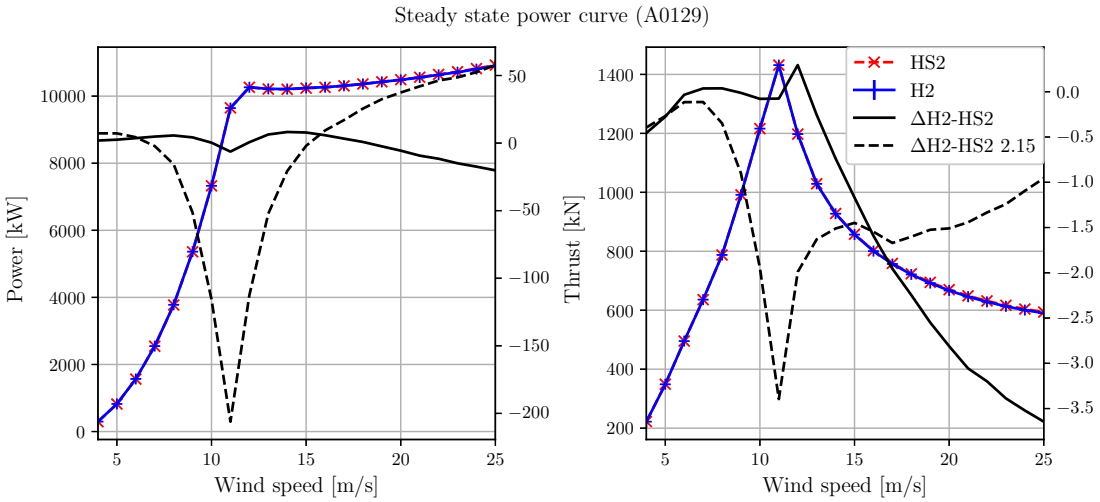

Figure 2.13: Power and thrust curves. The absolute difference between HAWC2 and HAWCStab2 is labelled as ΔH2-HS2, and its axis is on the right side of the plot.

The load distributions show similar trends compared to the stiff rotor (case 2, Figures 2.8 to 2.12). Without considering the detailed comparison of the blade deflection curves in this report (see section **??**), it seems that differences caused by the aerodynamics are minor, and they do not affect significantly the blade deformation.

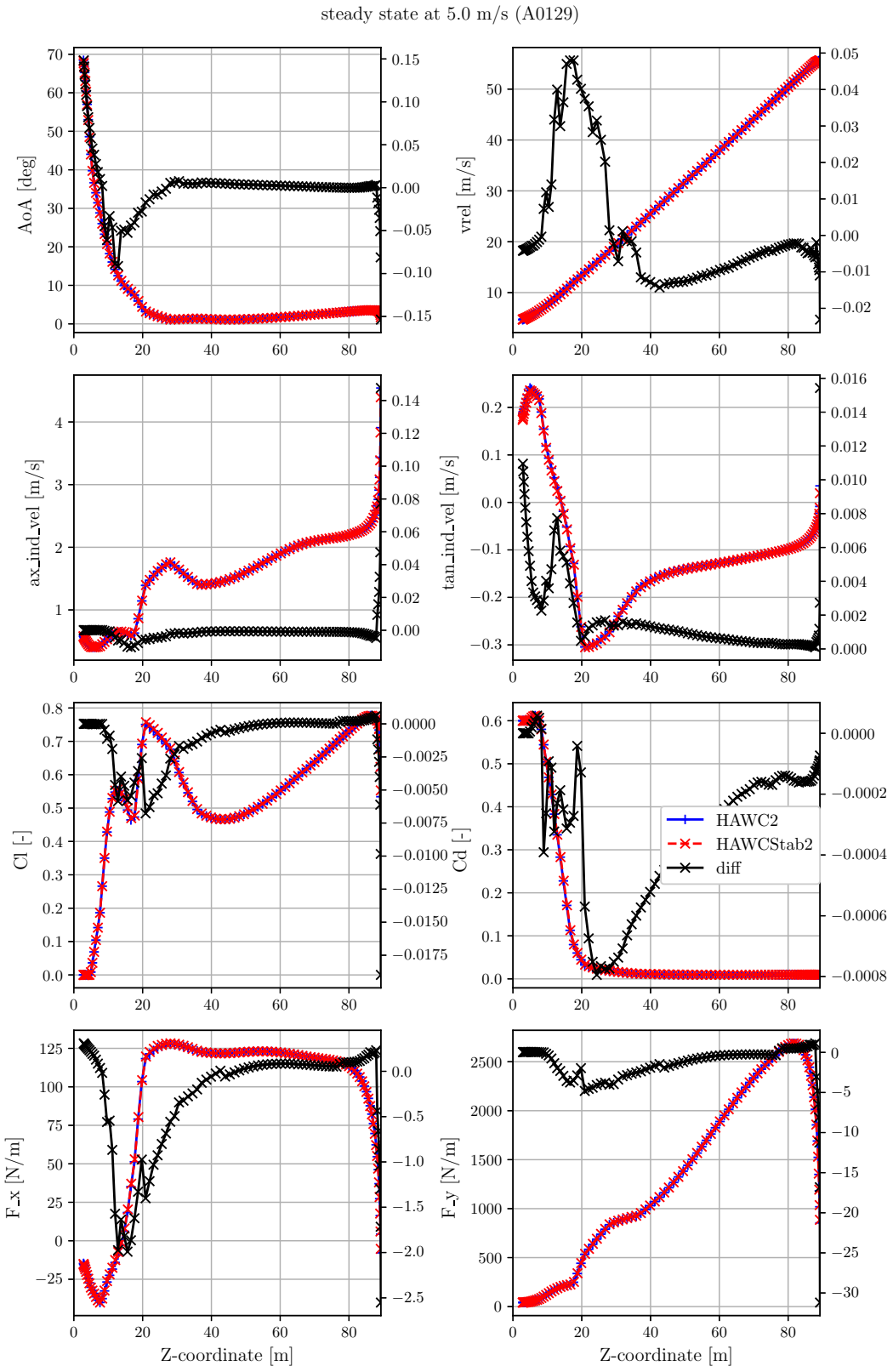

Figure 2.14: Blade load distribution at 5 m/s.

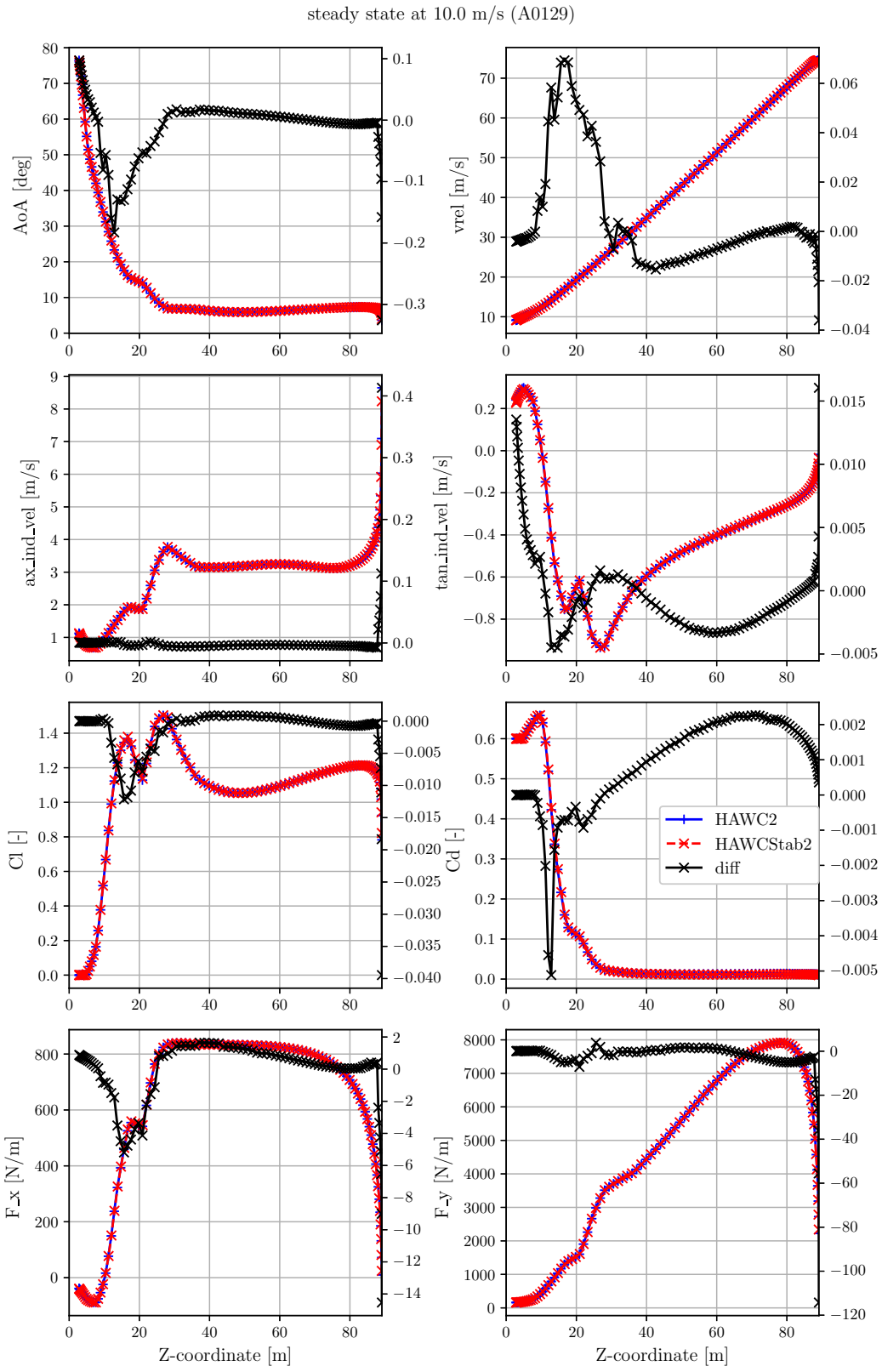

Figure 2.15: Blade load distribution at 10 m/s.

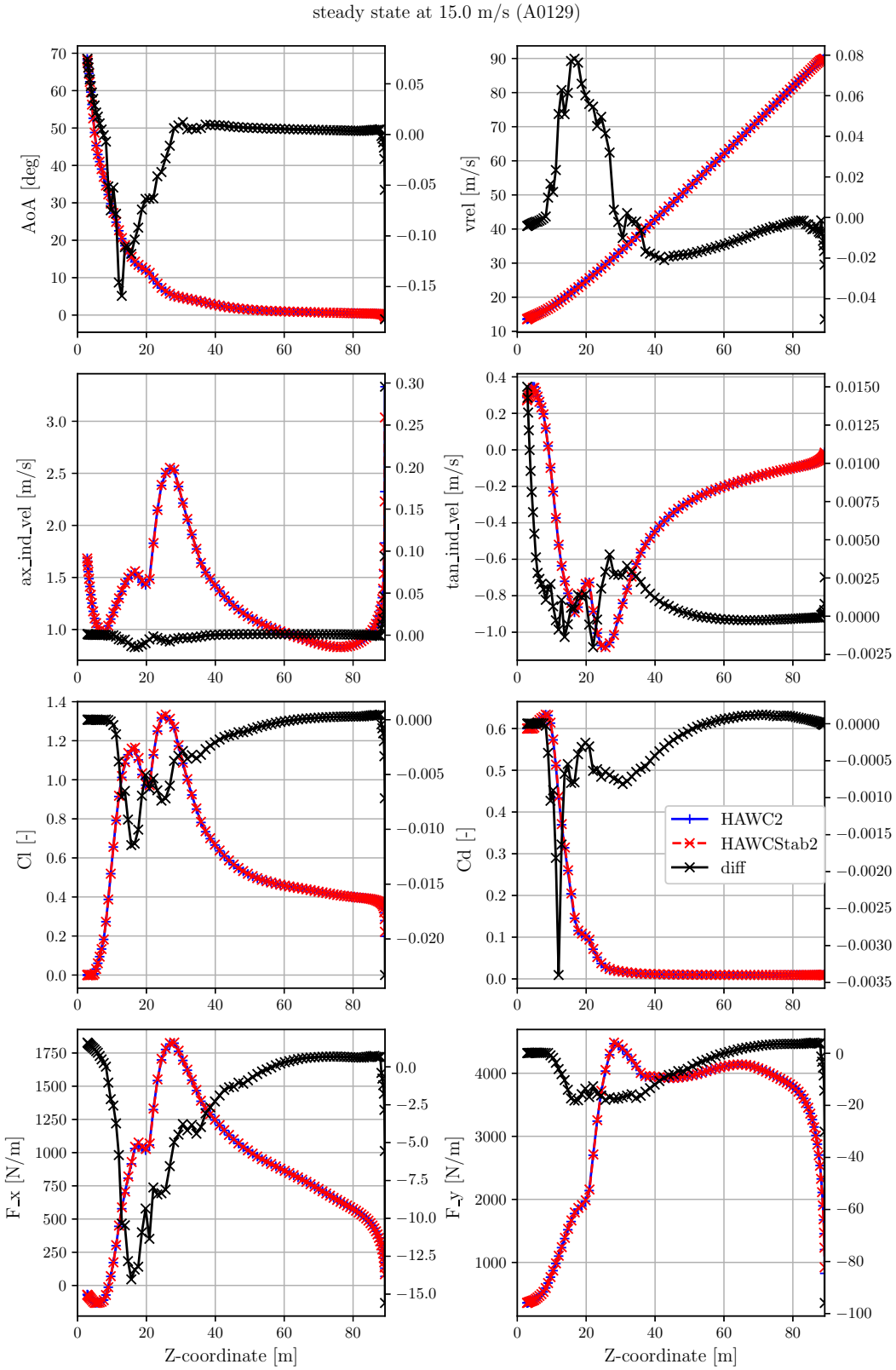

Figure 2.16: Blade load distribution at 15 m/s.

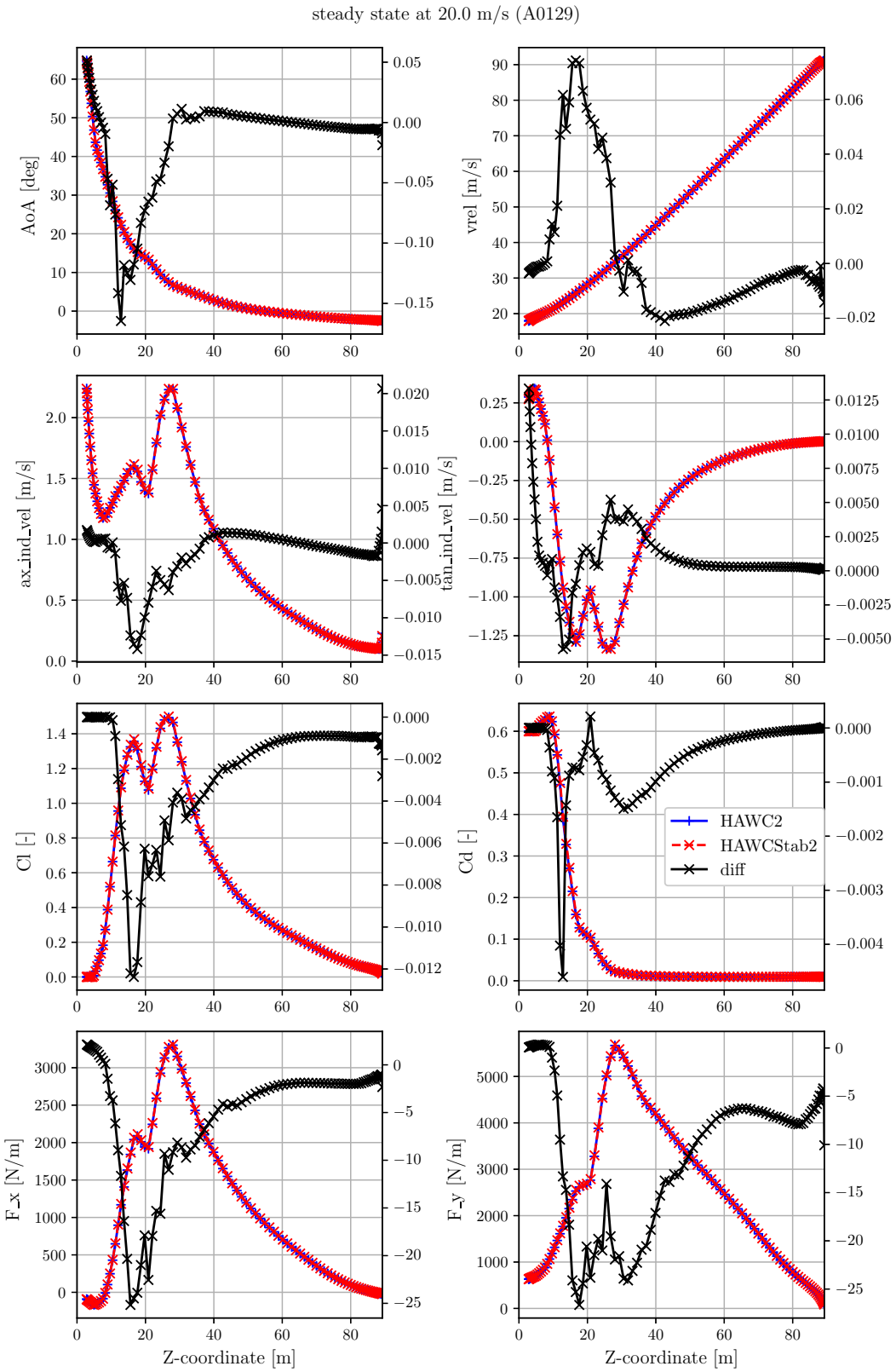

Figure 2.17: Blade load distribution at 20 m/s.

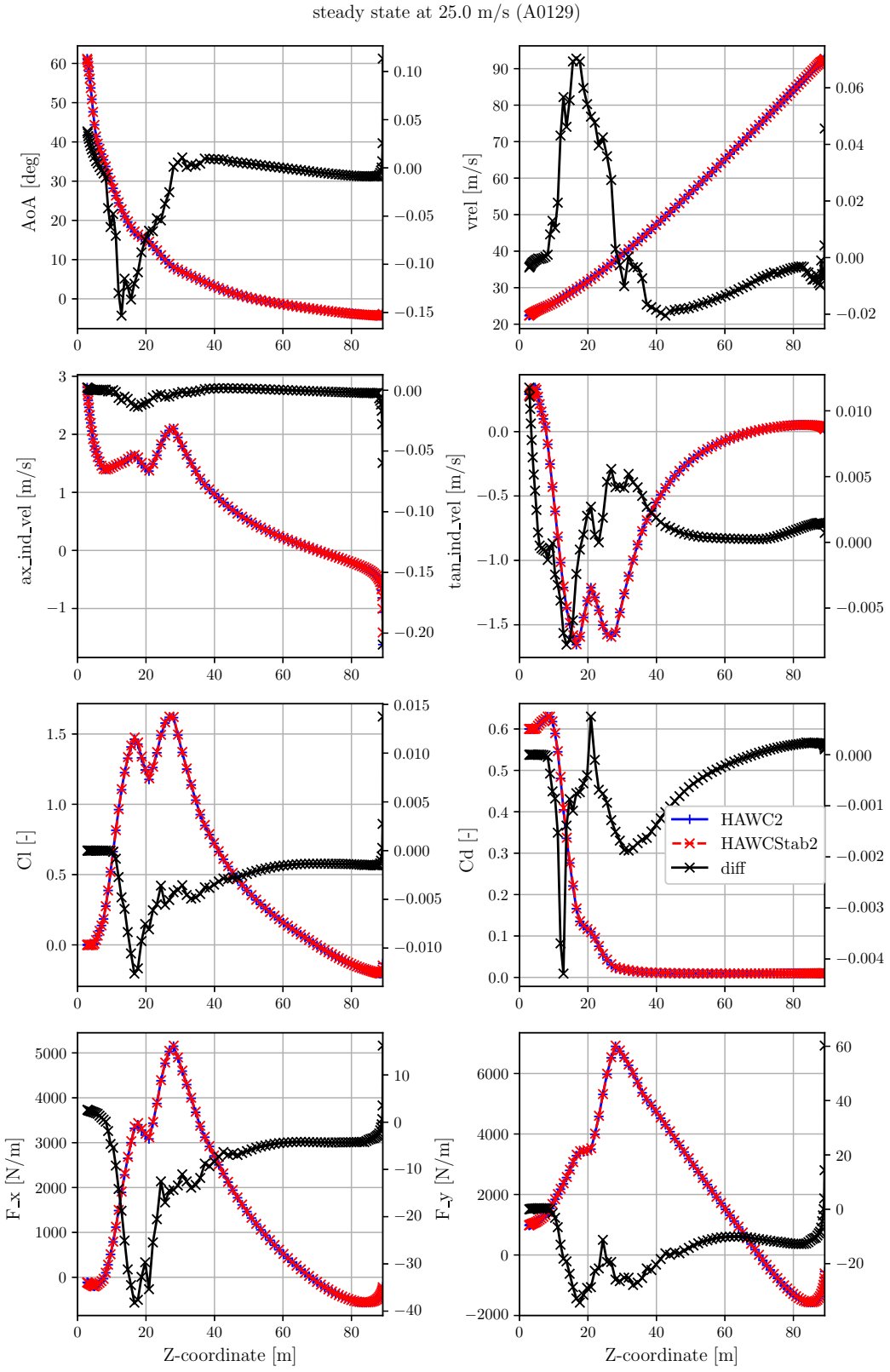

Figure 2.18: Blade load distribution at 25 m/s.

2.4 Case 4: flexible blades and “induction+tip” with 15 deg coning

This more challenging case was included to validate the aerodynamic modeling changes in the steady state computation in HAWCStab2 2.16. The power and thrust curves are shown in Figure 2.19. The maximum power deviation between HAWCStab2 2.16 and HAWC2 in this case is just above 1%, which is an error reduction by a factor of 4 compared to HAWCStab2 2.15. The maximum error in thrust is reduced by roughly a factor of 2. As observed in the previous section, HAWCStab2 2.15 compared well with HAWC2 12.6, which used an older aerodynamic model.

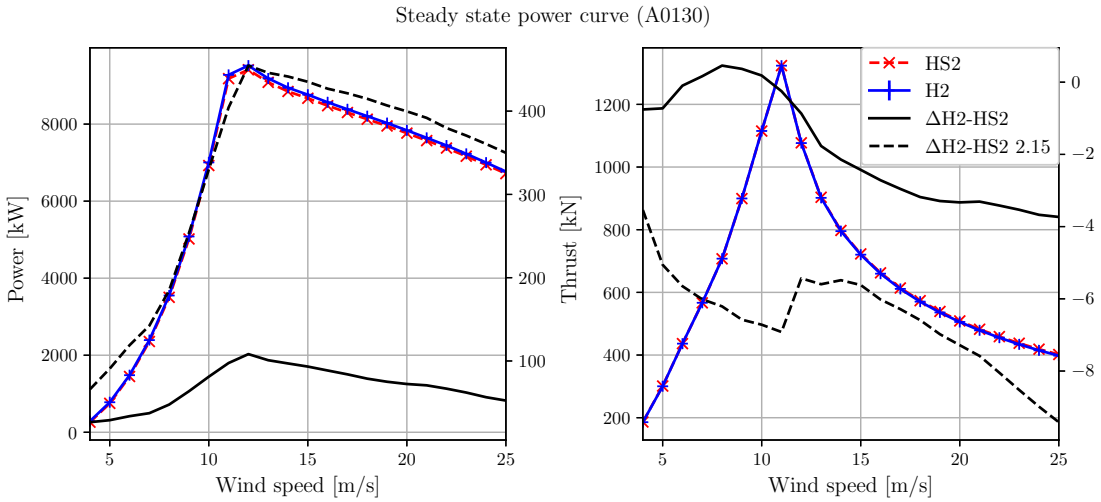

Figure 2.19: Power and thrust curves. The absolute difference between HAWC2 and HAWCStab2 is labelled as ΔH2-HS2, and its axis is on the right side of the plot.

The distributed aerodynamic parameters (Figures 2.20 to 2.23) are generally in good agreement, with the largest deviations at the blade root. There are slightly larger disagreements in the tangential velocity and drag coefficient up until roughly mid-blade, which need to be addressed in the future.

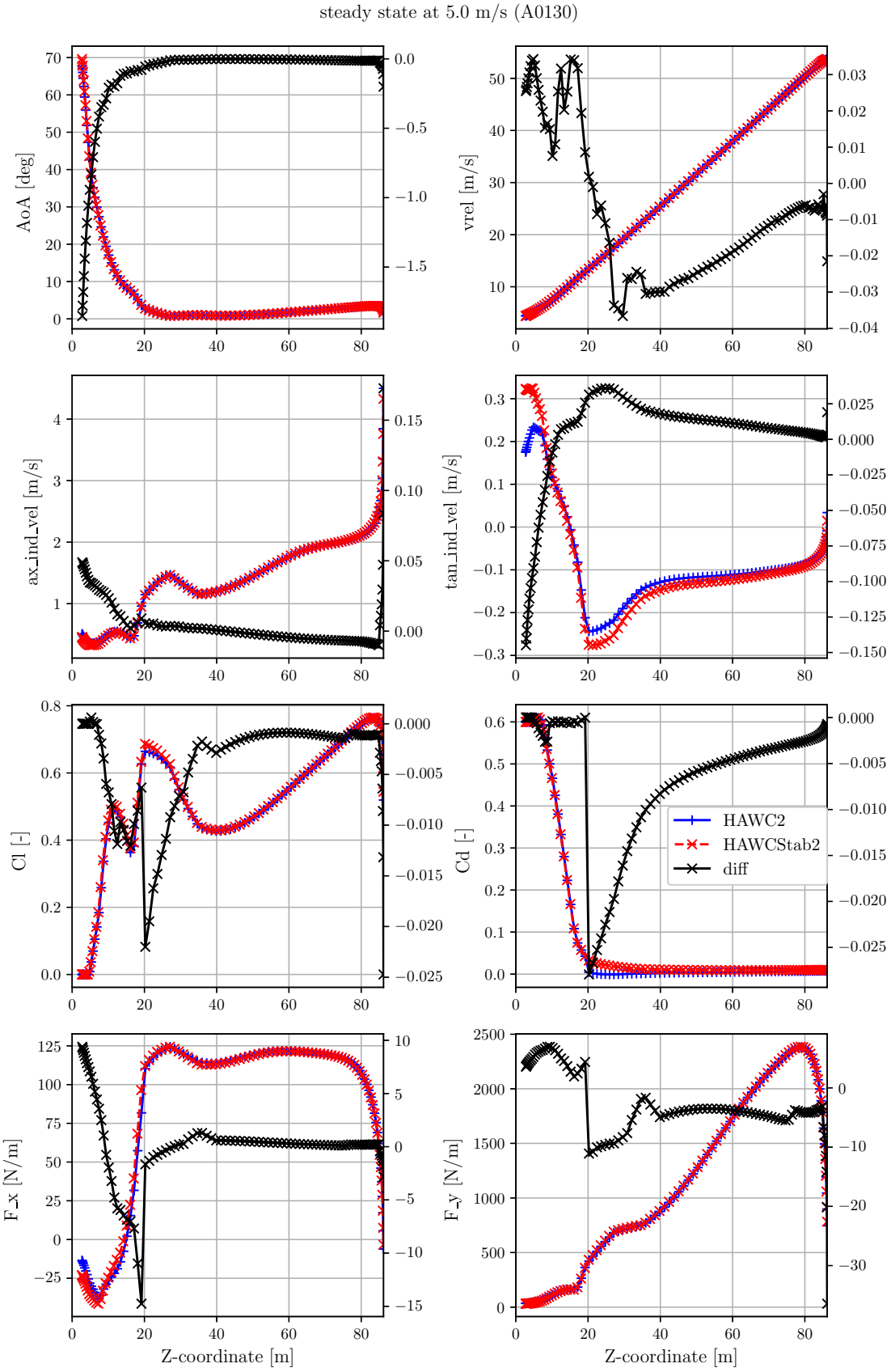

Figure 2.20: Blade load distribution at 5 m/s.

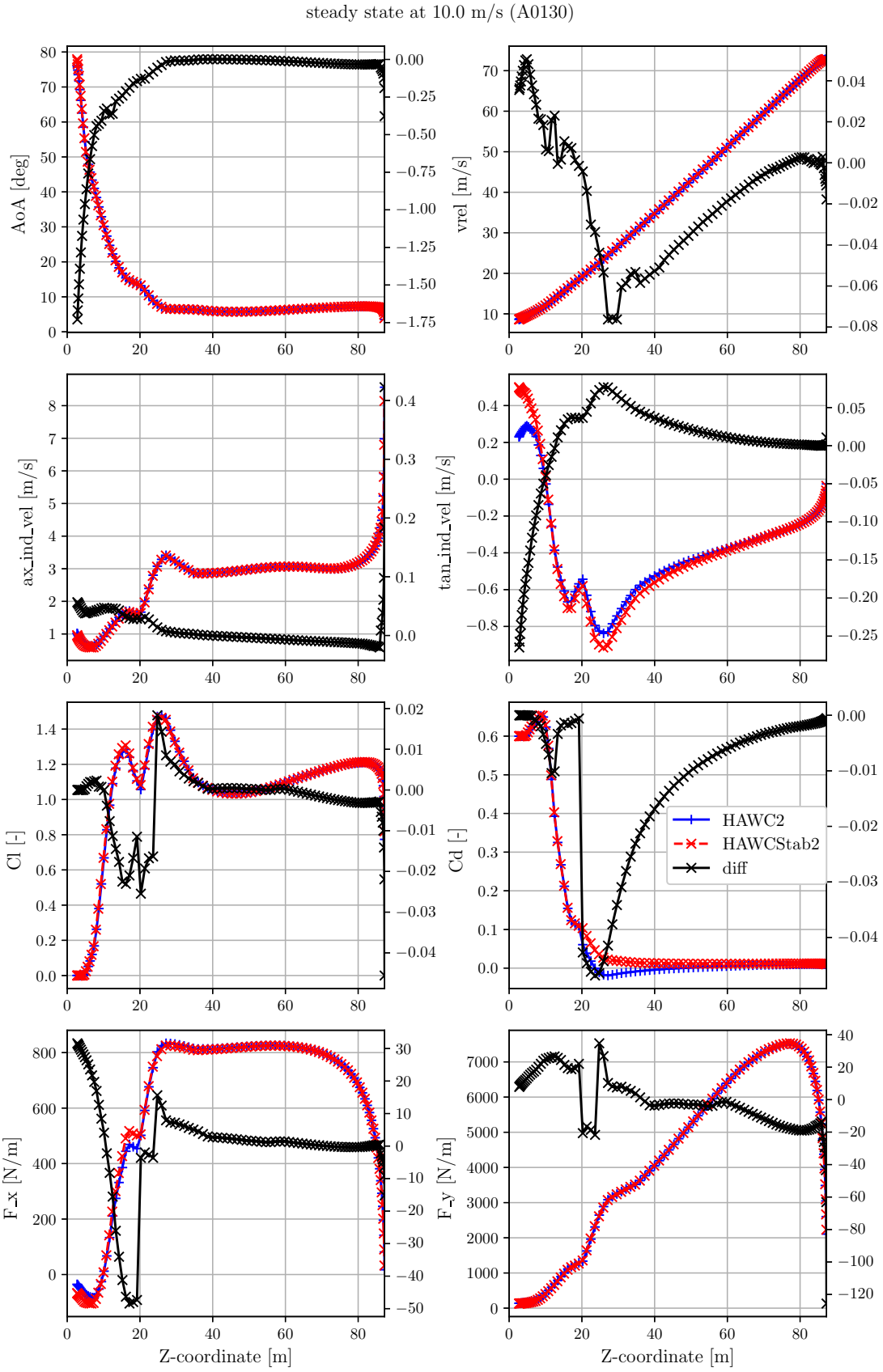

Figure 2.21: Blade load distribution at 10 m/s.

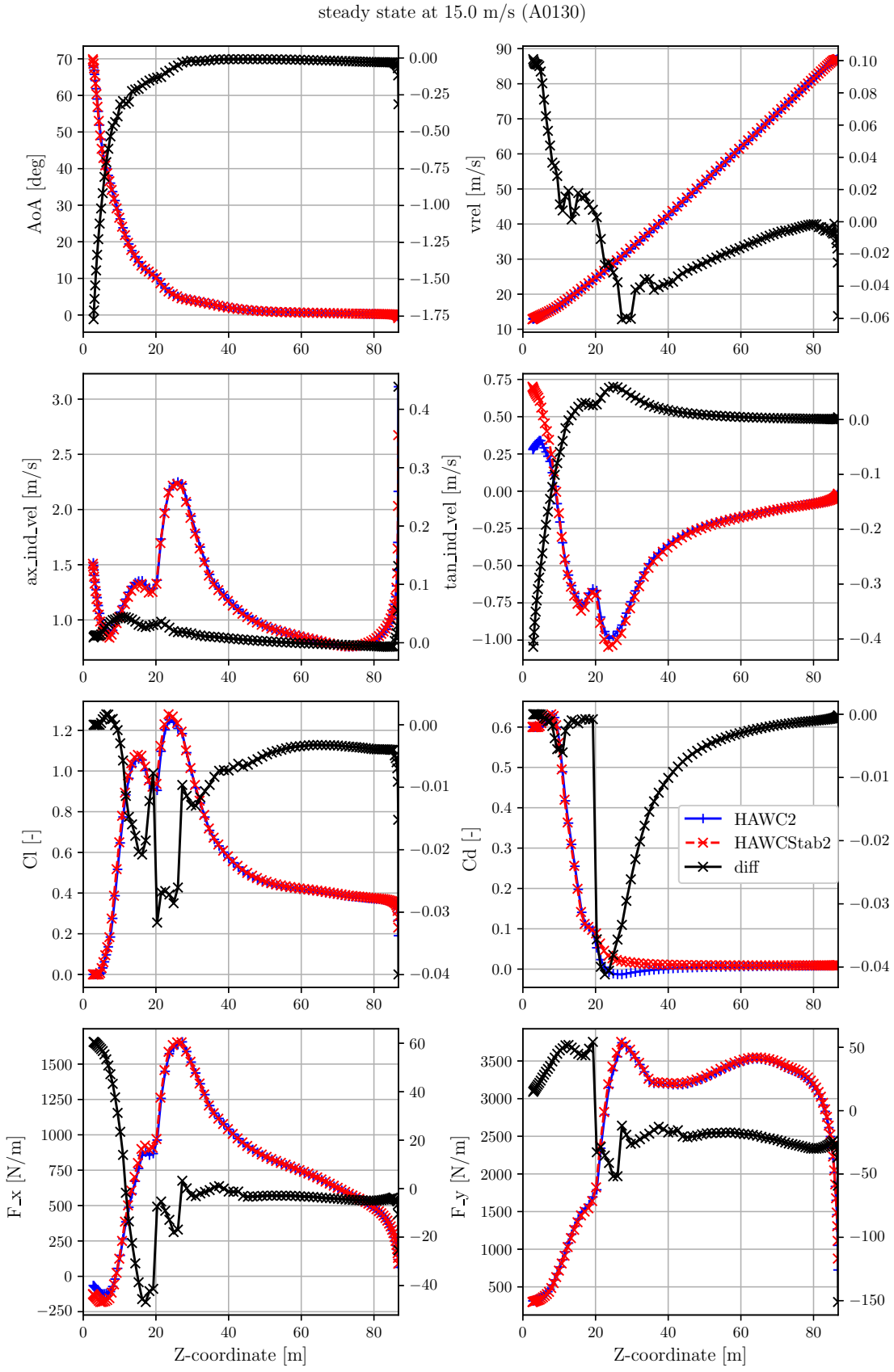

Figure 2.22: Blade load distribution at 15 m/s.

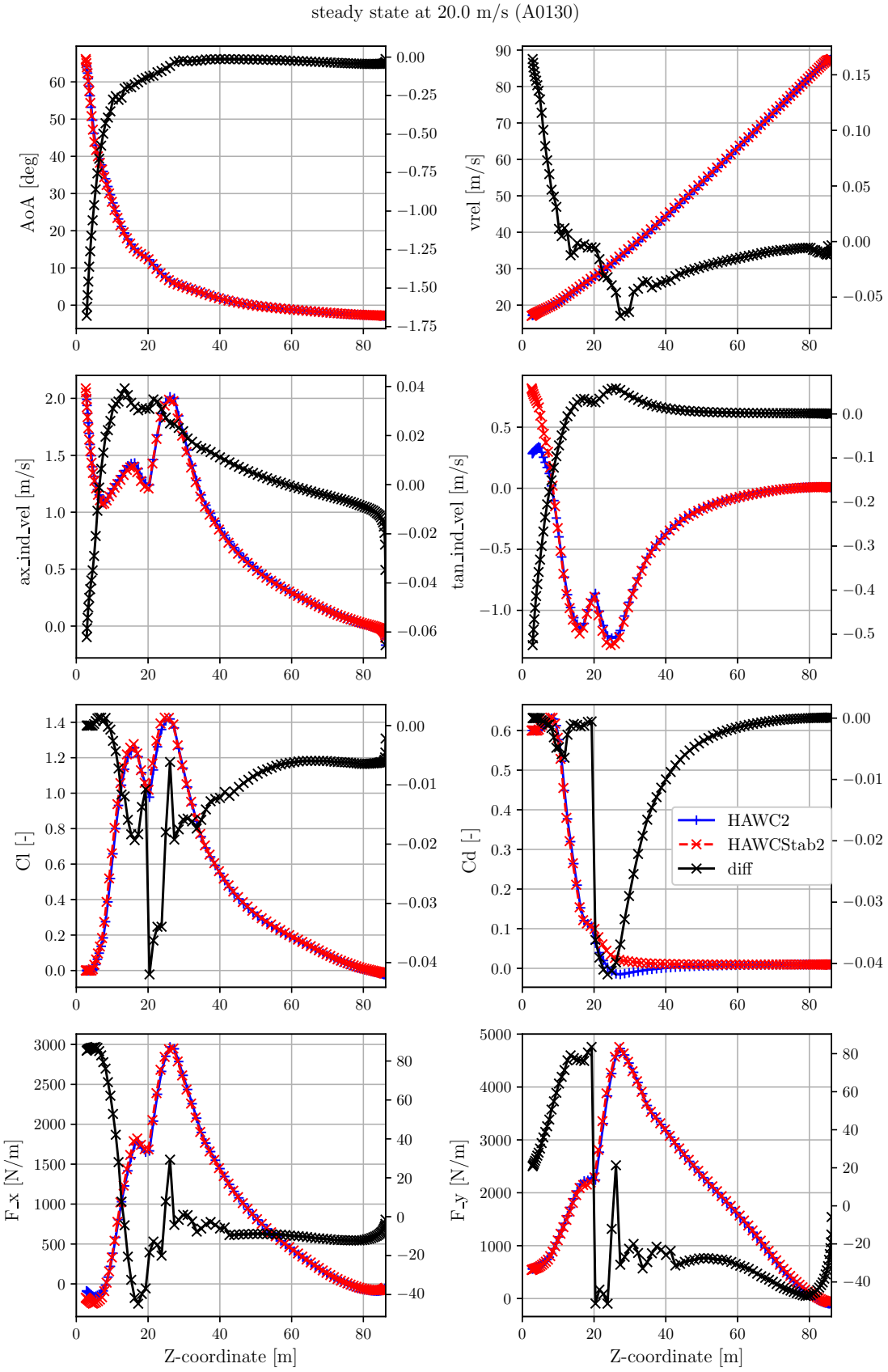

Figure 2.23: Blade load distribution at 20 m/s.

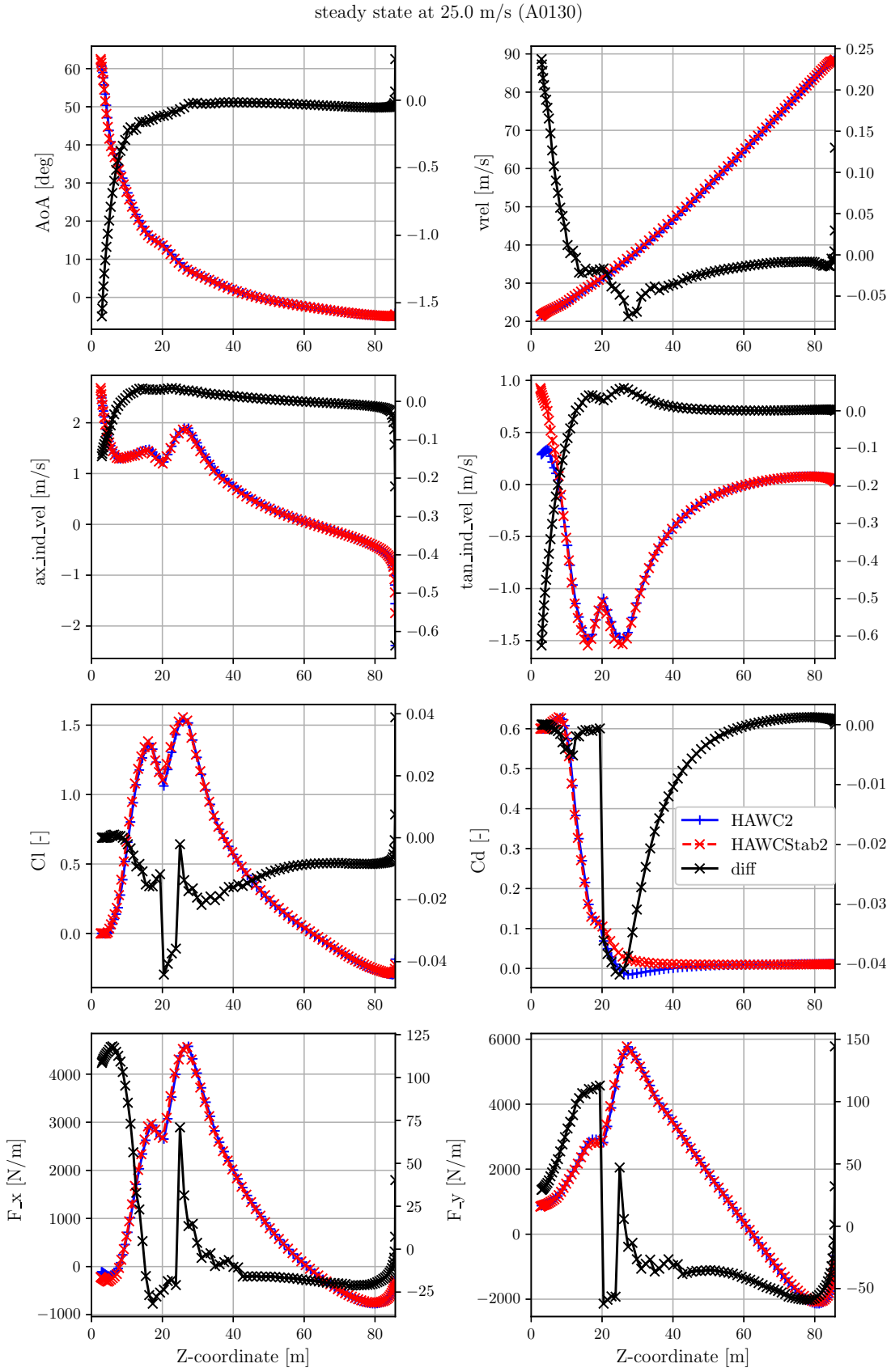

Figure 2.24: Blade load distribution at 25 m/s.

3 Blade structural eigenvalue analysis

In this section, we compare the structural eigenvalue analysis between HAWC2 and HAWCStab2 for the DTU 10 MW. The HAWCStab2 model does not include the pitch actuator, so that the blade modes are not altered by its low frequency. Moreover, the blade is non-rotating.

3.1 Classical Timoshenko beam and damping_posdef

For the first comparison we use the classical Timoshenko beam, with the damping_posdef damping model. Figure 3.1 shows the damped frequencies and Figure 3.2 the damping ratios. The comparison is good across HAWCStab2 2.15, 2.16 and HAWC2 13.1. Some small differences appear on the damping starting from the eighth mode.

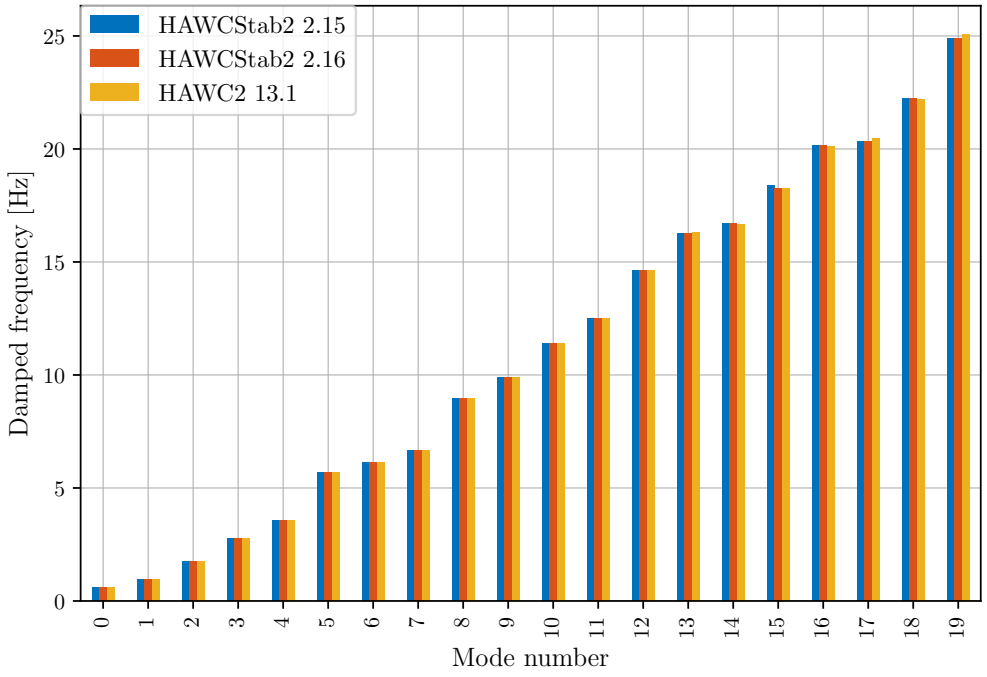

Figure 3.1: Structural damped frequencies of the non-rotating DTU 10 MW blade, with classical Timoshenko and damping_posdef.

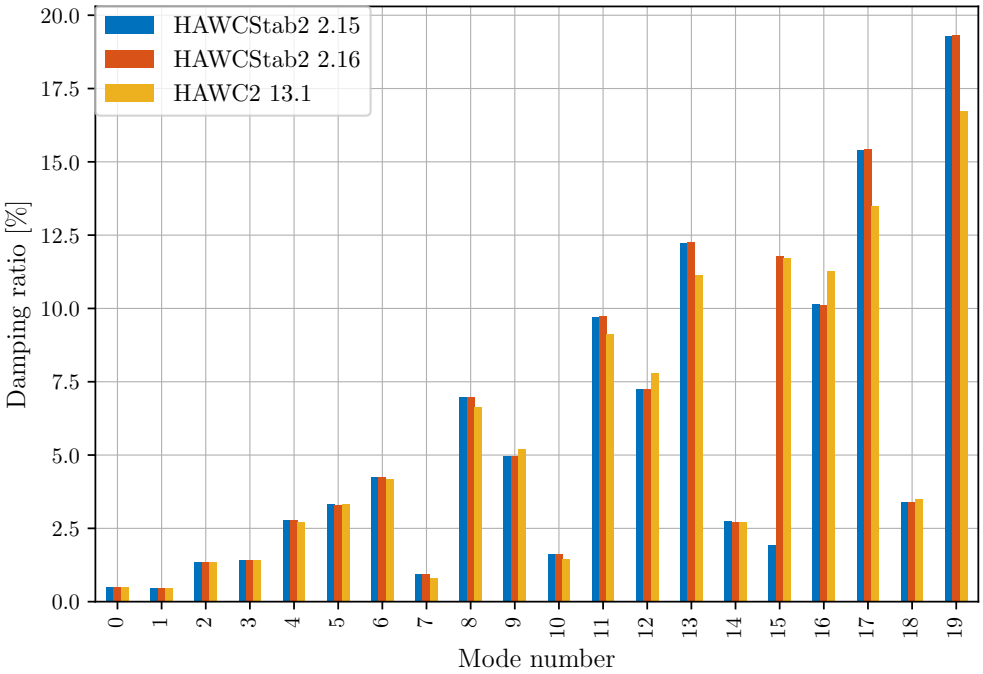

Figure 3.2: Structural damping ratios of the non-rotating DTU 10 MW blade, with classical Timoshenko and damping_posdef.

3.2 FPM beam and damping_aniso_v2

For the second comparison we have tested the new features of HAWCStab2 2.16. We have thus built the Fully-Populated Matrix (FPM) equivalent of the classical Timoshenko beam, and switched to the damping_aniso_v2 damping model. The result is shown in Figures 3.3 and 3.4. These new models show a better comparison between HAWC2 and HAWCStab2.

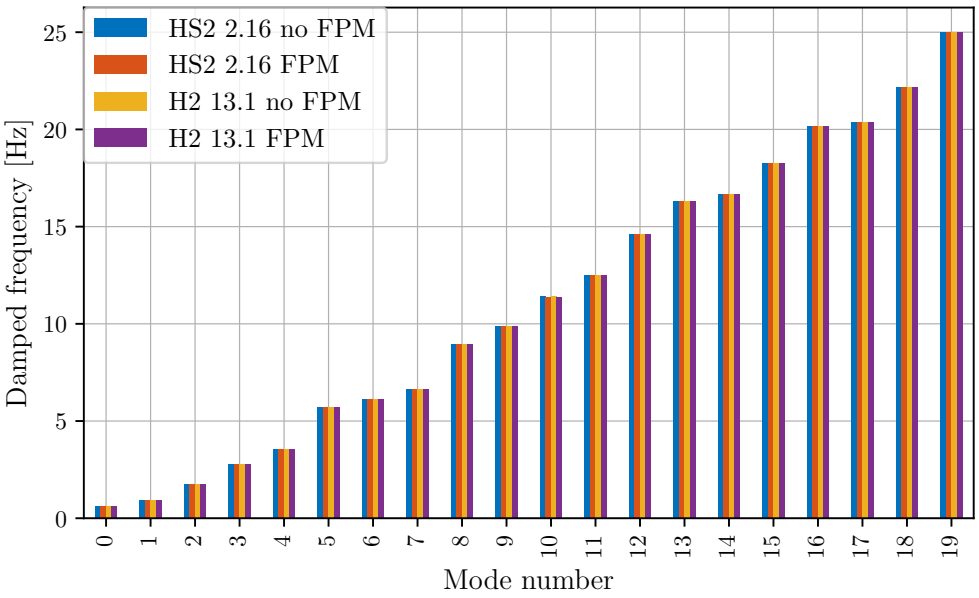

Figure 3.3: Structural damped frequencies of the non-rotating DTU 10 MW blade, with and without FPM and damping_aniso_v2.

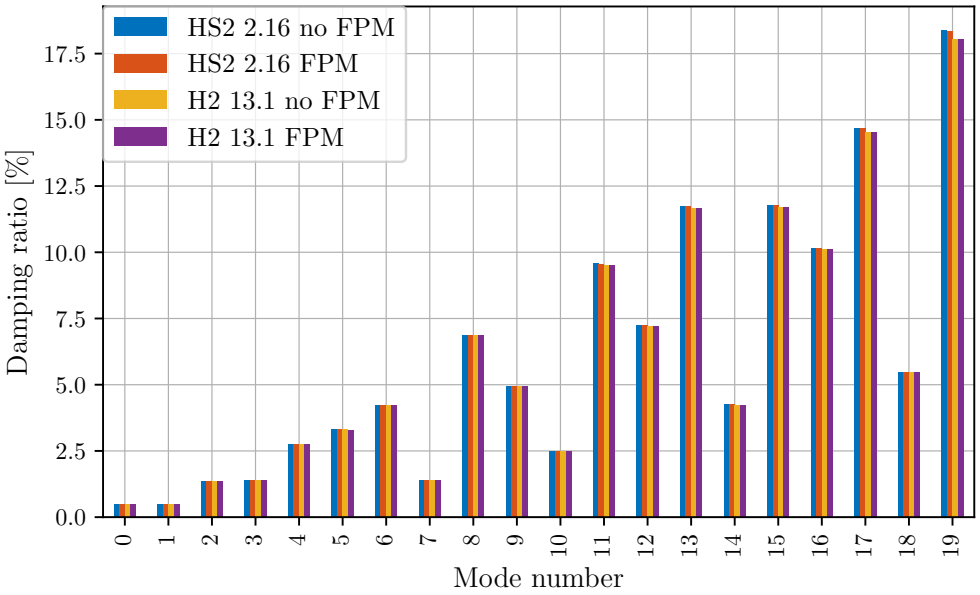

Figure 3.4: Structural damping ratios of the non-rotating DTU 10 MW blade, with and without FPM and damping_aniso_v2.

4 Conclusions

This report discussed the differences of the aerodynamic and aeroelastic performance and loading of the DTU 10 MW reference turbine using steady state results between HAWC2 and HAWCStab2. There is a consistently good agreement between HAWC2 and HAWCStab2 for both the rotor integrated forces as well as for the distributed blade performance parameters. A comparison of structural blade-only frequencies and damping ratios was also performed. The main conclusions are:

- Integrated rotor performance parameters (rotor power and thrust) differences are generally below 1%. An exception is the maximum power deviation of just above 1% for the 15 degree cone case.
- The modifications in the steady state aerodynamics in HAWCStab2 2.16 to improve the modelling of non-planar rotors, according to [8] and [11], have been successful. The maximum error in power compared to HAWC2 13.1 is reduced by a factor of roughly 10 in the standard aeroelastic case, and by a factor of roughly 4 in the aeroelastic case with 15 degrees cone.
- Distributed blade parameters show a small difference at the inboard sections, but the exact source of this discrepancy remains unclear. For the aeroelastic case with coning, there are slightly larger disagreements in the tangential velocity and drag coefficient up until roughly mid-blade, which need to be addressed in the future.
- The Prandtl tip correction model introduces a very small discrepancy at the tip. This issue is referred to future work.
- A comparison of the structural blade-only frequencies and damping ratios between HAWCStab2 and HAWC2 was performed. The frequencies are in excellent agreement in all cases. The damping ratios are in good agreement when the damping_posdef definition is used. With damping_aniso_v2, the agreement of the damping ratios is excellent.

Finally, it is concluded that the steady state performance computations of HAWCStab2 v2.16 are very close to the steady state simulation results of HAWC2 v13.1. Minor differences, who do not show to affect the steady state performance of the DTU 10 MW in a significant manner, are to be addressed in future version comparisons.

Bibliography

[1] Torben J. Larsen and Anders Melchior Hansen. *How 2 HAWC2, the user's manual (version 3-1)*. Report Risø-R-1597. Risø National Laboratory, 2007. URL: http://orbit.dtu.dk/en/publications/how-2-hawc2-the-users-manual(18aac953-55e6-4130-9b54-a6830618c5ca).html.

[2] Torben J. Larsen and Anders Melchior Hansen. *How 2 HAWC2, the user's manual (latest version)*. Report. URL: https://tools.windenergy.dtu.dk/home/HAWC2/.

[3] *HAWC2 website*. URL: https://www.hawc2.dk/.

[4] Bak, Christian. *The DTU 10-MW Reference Wind Turbine*. Fredericia, Denmark, 2013. URL: http://orbit.dtu.dk/en/publications/the-dtu-10mw-reference-wind-turbine(bc5f61cd-4c51-442f-89eb-02df89ab0aa4).html.

[5] M. H. Hansen. "Aeroelastic stability analysis of wind turbines using an eigenvalue approach". In: *Wind Energy* 7 (Apr. 2004). ISSN: 1099-1824. DOI: 10.1002/we.116. URL: http://onlinelibrary.wiley.com/doi/10.1002/we.116/abstract.

[6] M. H. Hansen. "Aeroelastic properties of backward swept blades". In: (2011). DOI: 10.2514/6.2011-260. URL: http://arc.aiaa.org/doi/abs/10.2514/6.2011-260.

[7] *HAWCStab2 website*. URL: https://www.hawcstab2.vindenergi.dtu.dk/.

[8] A. Li et al. "How should the lift and drag forces be calculated from 2-D airfoil data for dihedral or coned wind turbine blades?" In: *Wind Energy Science* 7.4 (2022), pp. 1341–1365. DOI: 10.5194/wes-7-1341-2022. URL: https://wes.copernicus.org/articles/7/1341/2022/.

[9] David Robert Verelst, Morten Hartvig Hansen, and Georg Pirrung. *Steady State Comparisons HAWC2 v12.2 vs HAWCStab2 v2.12*. English. Tech. rep. DTU Wind Energy, 2016. URL: https://orbit.dtu.dk/en/publications/steady-state-comparisons-hawc2-v122-vs-hawcstab2-v212 (visited on 02/09/2020).

[10] David Robert Verelst, Morten Hartvig Hansen, and Georg Pirrung. *Steady State Comparisons HAWC2 v12.5 vs HAWCStab2 v2.14: Integrated and distributed aerodynamic performance*. English. Tech. rep. DTU Wind Energy, 2018. URL: https://orbit.dtu.dk/en/publications/steady-state-comparisons-hawc2-v125-vs-hawcstab2-v214-integrated- (visited on 02/09/2020).

[11] H. A. Madsen et al. "Implementation of the blade element momentum model on a polar grid and its aeroelastic load impact". In: *Wind Energy Science* 5.1 (2020), pp. 1–27. DOI: 10.5194/wes-5-1-2020. URL: https://wes.copernicus.org/articles/5/1/2020/.

DTU Wind
Department of Wind and Energy Systems
Technical University of Denmark

RisøCampus Building 118
Frederiksborgvej 399
DK-4000 Roskilde
https://wind.dtu.dk/